View metadata, citation and similar papers at core.ac.uk

brought to you by CORE

provided by Carolina Digital Repository

HHS Public Access

Author manuscript

ACS Chem Biol. Author manuscript; available in PMC 2016 April 17.

Published in final edited form as:

ACS Chem Biol. 2015 April 17; 10(4): 1072–1081. doi:10.1021/cb500956g.

Identification of a Fragment-like Small Molecule Ligand for the Methyl-lysine Binding Protein, 53BP1

Michael T. Perfetti[1], **Brandi M. Baughma**[1], **Bradley M. Dickson**[1], **Yunxiang Mu**[2], **Gaofeng Cui**[3], **Pavel Mader**[4], **Aiping Dong**[4], **Jacqueline L. Norris**[1], **Scott B. Rothbart**[5], **Brian D. Strahl**[5], **Peter J. Brown**[4], **William P. Janzen**[1], **Cheryl H. Arrowsmith**[4], **Georges Mer**[3], **Kevin M. McBride**[2], **Lindsey I. James**[1], and **Stephen V. Frye**[1]

Lindsey I. James: ingerman@email.unc.edu; Stephen V. Frye: svfrye@email.unc.edu

[1]Center for Integrative Chemical Biology and Drug Discovery, Division of Chemical Biology and Medicinal Chemistry, UNC Eshelman School of Pharmacy, University of North Carolina at Chapel Hill, Chapel Hill, North Carolina 27599, USA

[2]Department of Molecular Carcinogenesis, University of Texas MD Anderson Cancer Center, Smithville, Texas, USA

[3]Department of Biochemistry and Molecular Biology, Mayo Clinic, Rochester, Minnesota, USA

[4]Structural Genomics Consortium, University of Toronto, Toronto, Ontario, Canada, M5G 1L7

[5]Department of Biochemistry and Biophysics, University of North Carolina at Chapel Hill, Chapel Hill, North Carolina 27599, USA

Abstract

Improving our understanding of the role of chromatin regulators in the initiation, development, and suppression of cancer and other devastating diseases is critical, as they are integral players in regulating DNA integrity and gene expression. Developing small molecule inhibitors for this target class with cellular activity is a crucial step toward elucidating their specific functions. We specifically targeted the DNA damage response protein, 53BP1, which uses its tandem tudor domain to recognize histone H4 dimethylated on lysine 20 (H4K20me2), a modification induced by double-strand DNA breaks. Through a cross-screening approach we identified UNC2170 (**1**) as a micromolar ligand of 53BP1, which demonstrates at least 17-fold selectivity for 53BP1 as compared to other methyl-lysine (Kme) binding proteins tested. Structural studies revealed that the *tert*-butyl amine of UNC2170 anchors the compound in the methyl-lysine (Kme) binding pocket of 53BP1, making it competitive with endogenous Kme substrates. X-ray crystallography also demonstrated that UNC2170 binds at the interface of two tudor domains of a 53BP1 dimer. Importantly, this compound functions as a 53BP1 antagonist in cellular lysates and shows cellular

Copyright © American Chemical Society.

Correspondence to: Lindsey I. James, `ingerman@email.unc.edu`; Stephen V. Frye, `svfrye@email.unc.edu`.

Supporting Information. Supporting figures and tables, a detailed description of the chemical synthesis and characterization, and the materials and experimental methods are described in the Supporting Information. This material is available free of charge via the Internet at http://pubs.acs.org.

Accession Codes. The structure of 53BP1 bound to UNC2170 (**1**) has been deposited with the Protein Data Bank as entry 4RG2.

The authors declare no competing financial interest.

Author Manuscript

Author Manuscript

Author Manuscript

Author Manuscript

Author Manuscript Author Manuscript Author Manuscript Author Manuscript

activity by suppressing class switch recombination, a process which requires a functional 53BP1 tudor domain. These results demonstrate that UNC2170 is a functionally active, fragment-like ligand for 53BP1.

One of the major processes regulating gene expression is the dynamic control of chromatin architecture. A key mechanism involved is the addition, recognition, and removal of post-translational modifications (PTMs) on histone proteins by various enzymes and binding proteins.(1) In particular, the recognition of methylated lysine residues on histone tails by methyl-lysine (Kme) binding proteins is a critical event in chromatin regulation.(2, 3) These binding events recruit effector proteins and their macromolecular complexes to support defined gene activation and repression outcomes. Importantly, histone Kme binding has been shown to be misregulated in diseases including cancer and is essential to critical cellular processes such as DNA damage repair.(4–6)

53BP1 is a Kme binding protein that plays a central role in DNA Damage Repair (DDR) pathways and is recruited to sites of double-strand breaks (DSB). This process is dependent on the activity of ataxia telangiectasia mutated (ATM) kinase that regulates the DNA damage signaling response. Recruitment of 53BP1 can lead to cell cycle arrest and DNA damage repair, or lack thereof if there are defects or deficiencies present in the enzymes or proteins involved in this signaling cascade.(7–19) Cells deficient in 53BP1 prove to be viable but display a phenotype resembling mild ATM kinase-signaling defects due to the cell's inability to properly respond to and repair DNA damage.(20, 21) 53BP1 knockout mice are viable, but are growth retarded, immune deficient, radiation sensitive, and cancer prone.(20) In addition, these mice display a defect in antibody class switch recombination (CSR) which also requires 53BP1 activity.(22) By testing different fragments of the 53BP1 gene, it has been shown that the region that harbors its Kme binding tandem tudor domain (amino acids 1235–1709) is recruited to ionizing radiation (IR)-induced foci as efficiently as full-length, endogenous 53BP1.(23) Histone H4 lysine 20 dimethyl (H4K20me2) was identified as the primary PTM in histones recognized by the 53BP1 tandem tudor domain (TTD),(24) and this finding was subsequently supported by structural studies.(25) Additionally, the TTD of 53BP1 has been shown to bind to p53K382me2 and thereby increase the concentration of p53 at DNA damage sites.(26) Unlike H2AX phosphorylation, global levels of H4K20me2 do not increase after DNA damage; instead, 53BP1 recognizes histone H2A ubiquitylated at lysine 15 by RNF168 in response to DNA double-strand breaks.(27) 53BP1 recruitment is also facilitated by RNF168 ubiquitylation-dependent removal of L3MBTL1 and JMJD2A from H4K20me2 after DNA damage.(28, 29)

BRCA1 is a checkpoint and DNA damage repair gene that is required for maintenance of genomic integrity, and the inheritance of mutated *BRCA1* is a major risk factor for breast and ovarian cancer.(30) BRCA1 knockout in mice is embryonic lethal,(31) and conditional knockout in the mammary gland results in low frequency and long latency of mammary tumor formation.(32) It was recently reported that the BRCA1 knockout developmental phenotype is rescued when placed on a 53BP1-null background, and adult mice that are null for both the *53BP1* and *BRCA1* genes age normally and display a very low incidence of tumor formation.(33) The genomic instability in the BRCA1 knockout can be overcome

Author Manuscript Author Manuscript Author Manuscript Author Manuscript

because the homologous recombination (HR) pathway is largely restored in cells lacking both BRCA1 and 53BP1.(34)

We hypothesized that a small molecule ligand that prevents Kme recognition by 53BP1 would antagonize its biological activity in cells possessing BRCA1 mutations and lead to rescue of their genomic stability by restoration of the HR pathway. Notwithstanding the clinical challenges of cancer prevention strategies, the discovery of a small molecule *in vivo* probe for 53BP1 would enable this hypothesis to be tested preclinically, and the devastating effects of *BRCA1* mutations, including prophylactic surgical interventions,(21) could perhaps be diminished. We therefore aimed to synthesize cell penetrant small molecules that would bind selectively to the tandem tudor domain of 53BP1 using structure-based design and iterative medicinal chemistry. Herein we report the initial results of this effort.

RESULTS AND DISCUSSION

A structure-based design approach was initiated by analyzing available crystal structure data of 53BP1 bound to an H4K20me2 peptide (PDB 2IG0).(25) The key interactions noted in this structure were a hydrogen-bond between the Kme basic amine and an aspartic acid (Asp1521), cation-π interactions between Kme2 and phenylalanine, tyrosine, and tryptophan residues within the aromatic binding cage (Tyr1502, Tyr1523, Phe1519, Trp1495), and a cation-π interaction between arginine 19 on the H4 peptide tail and a tryptophan residue (Trp1500).(25) Mutagenesis of the histone peptide had previously demonstrated that H18 also contributes to binding, but this interaction was not clearly defined in the X-ray crystal structure.(25) To develop a more complete understanding of the binding interactions of the H4 peptide (amino acids 14–27) bound to 53BP1, isotope enriched (^{13}C and ^{15}N) NMR spectroscopy(35) was applied to determine the structure of the central residues of the H4K20me2 peptide bound to 53BP1 (PDB 2LVM).(36) It was observed that this central region of the H4 peptide corresponding to residues 15 to 22 adopts a “U-turn” conformation. Notably, in addition to the binding interactions with H4K20me2 and H4R19 that were detected in the crystal structure, further analysis revealed a pocket containing both acidic and hydrophobic residues that accommodates H4R17 and H4V21. It has also been shown that acetylation of H4K16 diminishes 53BP1 binding by disrupting a salt bridge between H4K16 and Glu1551.(36) Therefore, a small molecule that could occupy the methyl-lysine binding cage of 53BP1 and interact favorably with some of the surrounding residues would be expected to block 53BP1 binding to H4K20me2.

Our current efforts utilize a comprehensive cross-screening approach in order to evaluate all synthesized ligands against a panel of Kme reader domains. The Kme reader panel consists of 10 reader proteins from four different families: tudor domains (53BP1, UHRF1, PHF1, PHF19), chromodomains (CBX7), MBT domains (L3MBTL1, L3MBTL3, MBTD1), and PHD fingers (JARID1A, PHF23, UHRF1). These proteins were chosen largely based on available structural information, reader family representation, and biological relevance. Previously our lab reported an AlphaScreen bead-based proximity assay for Kme readers(37) and this screening tool was employed to initially assess 53BP1 binding. UNC2170 (**1**, Table 1) emerged as a preliminary 53BP1 hit from these cross-screening efforts. Because of the modest affinity of **1** (29 ± 7.4 μM) and its fragment-like nature (MW

Author Manuscript Author Manuscript Author Manuscript Author Manuscript

= 313.24, ligand efficiency = 0.35, lipophilic ligand efficiency = 1.5)(38, 39), we profiled it at concentrations up to 500 μM versus our reader panel to better ascertain its selectivity, as this is of paramount importance for chemical probe development (Supplementary Figure S1).(40) This revealed promising levels of selectivity within this small but diverse sampling of Kme reader proteins, as **1** showed no affinity within the concentrations tested against any other members of the panel, including other tudor domain containing proteins and other readers of methylated H4K20 (Table 1). Additionally, isothermal titration calorimetry (ITC) experiments confirmed ligand binding, revealing a K_d of 22 ± 2.5 μM for UNC2170 against the 53BP1 tandem tudor domain (Figure 1).

Based on this initial data, we initiated synthetic efforts to prepare analogues of UNC2170 in order to evaluate structure-activity relationships (SAR) within this series and improve the affinity for 53BP1. For these SAR studies, all synthesized ligands were tested at concentrations up to 100 μM against our Kme panel to evaluate both their selectivity and potency. Analysis of UNC2170 suggested three primary areas for synthetic modification: the basic amine, the linker region, and the aromatic ring. SAR for each of these regions are discussed below.

It was hypothesized that the basic amine of UNC2170 would bind within the Kme binding pocket of 53BP1, similar to dimethyl-lysine. Exploration of the steric tolerance of the basic amine in **1** began by replacement of the secondary *N*-*tert*-butyl amine group with dimethyl amine (**2**) to more closely mimic the endogenous H4K20me2 substrate (Table 1). Interestingly, this compound showed no binding activity by AlphaScreen and this finding was confirmed by ITC (Supplementary Figure S2).

This result led us to hypothesize that the 53BP1 Kme binding pocket may have a preference for secondary amines over tertiary amines in the context of the UNC2170 framework, in contrast to its preference for dimethylated versus monomethylated lysine peptides.(25) Preparation of the isopropyl amino compound, **3**, showed no activity against 53BP1 but interestingly, it was weakly active against some of the other tudor domain containing proteins in the panel (Table 1). Incorporation of other tertiary amines as in compound **4**, where the secondary amine of UNC2170 is methylated, also showed no appreciable binding activity up to 500 μM as measured by AlphaScreen (Table 1 and Supplementary Figure 1a). ITC studies further confirmed that **4** has no measurable affinity for 53BP1, and therefore compound **4** (UNC2892) was selected as a negative control compound due to its inactivity and structural similarity to UNC2170 (**1**).

Further exploration of the ligand tolerance within the Kme binding pocket by replacement of the basic amine with an oxygen (**5**) resulted in no activity, as anticipated. We also investigated whether 53BP1 has similar Kme mimetic preferences as the MBT containing protein, L3MBTL1, as both bind the H4K20me2 mark. Compounds incorporating pyrrolidine have been shown to serve as effective ligands for such MBT domain containing proteins.(41–45) To test this we introduced a pyrrolidine amine to give compound **6** and found that this modification did not improve affinity towards 53BP1, confirming that Kme readers of the same histone mark do not necessarily have similar small molecule ligand preferences. Overall, our SAR exploration of the basic amine of UNC2170 (**1**) shows that a

Author Manuscript Author Manuscript Author Manuscript Author Manuscript

sterically bulky, lipophilic secondary amine is preferred for binding in the Kme pocket of 53BP1.

Prior to expanding our SAR studies to other portions of the molecule, we first sought to confirm that the *N*-*tert*-butyl amine of UNC2170 (**1**) was mimicking the endogenous Kme2 ligand and binding within the Kme binding pocket. We prepared an active site mutant of 53BP1 (D1521A) that no longer binds H4K20me2 due to loss of a salt bridge and hydrogen bond with Asp1521.(25) ITC demonstrated that binding of UNC2170 (**1**) was abrogated by the 53BP1 D1521A mutant (Supplementary Figure S2) which is consistent with the basic amine of UNC2170 (**1**) occupying the Kme reader pocket.

Various linkers to modify the distance and flexibility between the basic amine of UNC2170 and the aromatic functional group were explored next (Table 2). Initial SAR efforts began with the substitution of a sulfonamide linker for the amide bond to give compound **7**, resulting in loss of 53BP1 binding affinity. Conversion of the amide to a benzylamine as in compound **8** similarly abrogated binding. When the linker region between the amide bond and basic nitrogen was rigidified using two different cyclic variants (compounds **9** and **10**), 53BP1 activity was again lost. Additionally, lengthening the aliphatic chain between the amide bond and the amine as in compounds **11** and **12** resulted in inactivity, while shortening the linker (**13**) had a similar effect. Within this series, the propyl alkyl chain in compound **1** was found to be optimal.

We extended our SAR studies to the aromatic ring of UNC2170 by first assessing the contribution of the bromine to binding via preparation of compound **14**, which showed no measurable binding to 53BP1 (Table 3). Furthermore, the bromine regioisomers, compounds **15** and **16**, were similarly inactive, suggesting that the bromine of UNC2170 is making a specific interaction with 53BP1. A halogen scan demonstrated that chlorine (**17**) and fluorine (**18**) provided no improvement in affinity, but replacement of the bromine with iodine was well tolerated (**19,** IC_{50} = 13 ± 4.8 μM). Consistent with this, we found that binding affinity is maintained when an isopropyl group (**20**) or a trifluoromethyl substituent (**21**) occupies the 3-position, suggesting that larger, more lipophilic substituents are preferred. The binding of **21** to 53BP1 was further confirmed by ITC (Supplementary Figure S2), which resulted in a K_d that correlated well with the AlphaScreen results (K_d = 10 ± 1.0 μM). While the 3-trifluoromethyl analog was roughly equipotent to UNC2170 (**1**), activity was also specific to this regioisomer, as compound **22** with CF_3 para to the amide is inactive. Replacement of the Br of **1** with a nitro group at the 3-position (**23**) also results in a loss in potency.

We hypothesized the halogenated 4-substituted pyridine derivatives, compounds **24** and **25**, would increase the positive charge of the σ-hole of the bromine in UNC2170 and the CF_3 in compound **21**, in turn both increasing the likelihood of a halogen-hydrogen bond with the protein and improving binding.(46) These pyridine analogs resulted in a decrease in potency relative to their phenyl counterparts, suggesting that a potential halogen bond with 53BP1 is unlikely and instead favorable hydrophobic interactions are contributing to binding.

Author Manuscript Author Manuscript Author Manuscript Author Manuscript

A number of other modifications to the aromatic ring were tested, including the addition of amino and hydroxyl groups at the 2-, 4-, and 5-positions while maintaining a 3-bromo substituent. UNC2170 derivatives incorporating functionalized lactones, furans, benzofurans, and pyridines, as well as variable methylene linkers between the amide bond and aromatic ring were also prepared. All of these analogs resulted in compounds that were inactive against 53BP1. Overall, these findings demonstrate that limited manipulations can be performed to the aromatic core of UNC2170 while maintaining potency, and that 53BP1 generally prefers analogs of UNC2170 that possess a lipophilic substituent at the 3-position.

To better understand the structural basis for UNC2170 binding, we co-crystallized the 53BP1 tandem tudor domain with UNC2170 and solved its structure by X-ray crystallography at 1.5 Å resolution (PDB 4RG2). Interestingly, we found that under these conditions UNC2170 is bound to a 53BP1 dimer, making distinct interactions with both tudor domains (Figure 2a). This correlates well with the molar ratio observed by ITC (Figure 1), which consistently produced an N value less than 1, suggesting a 2:1 ratio of protein to ligand. The structure revealed that the *N*-*tert*-butyl amine of UNC2170 is buried in the Kme binding pocket of one tudor domain (Figure 2b; magenta), driven largely by van der Waals interactions, hydrogen bonds, and electrostatic interactions. Due to the fact that the aromatic residues of both Kme pockets are greater than 5 Å from the amine, we anticipate that cation-π interactions are a minor contribution to binding relative to the hydrogen bonds formed between the ligand and protein.

The basic amine of UNC2170 is about equidistant from Asp1521 in each protein binding pocket (2.8 Å and 2.6 Å), and is well positioned to interact with and make a critical hydrogen bond to Asp1521 in both proteins. The importance of this interaction is consistent with ITC data that shows that the Kme pocket mutant, D1521A, does not bind to UNC2170. Additionally, the amide nitrogen is also within hydrogen bonding distance of the Asp1521 residue of one tudor domain, which is likely to further facilitate binding. The distance between the amine and the amide of UNC2170 therefore appears to be quite important in enabling a number of key interactions, and this sheds light on why changing the length of the aliphatic linker (compounds **11** – **13**) impairs binding. The aliphatic linker and aromatic ring of UNC2170 is also nicely sandwiched between the dimer interface, packing against the surface of each protein unit.

Various series of analogs were prepared around UNC2170 beyond those presented above, many of which contained less subtle modifications; however, they all revealed a minimal tolerance to modification of the original ligand structure. The co-crystal structure assists in explaining this lack of SAR, as the interaction of UNC2170 with the 53BP1 dimer reveals that the ligand is encircled by both proteins and that there is limited space for modification. This is in contrast to our preliminary structural predictions based on UN2170 bound to a single 53BP1 tudor domain. We plan to utilize this novel binding mode in future efforts aimed at designing both UNC2170 related and structurally distinct inhibitors of 53PB1.

In addition to the X-ray structure, a ^{1}H-^{15}N HSQC NMR correlation spectrum of the tudor domain of 53BP1 was also obtained in the absence and presence of a 10-fold excess of UNC2170. Extensive changes in chemical shifts were observed (Figure 2c), further

Author Manuscript Author Manuscript Author Manuscript Author Manuscript

confirming specific binding of the ligand to 53BP1. Exchange between the bound and unbound state was observed to be slow on the NMR chemical shift time scale which is surprising given the measured affinity of UNC2170.

To further evaluate whether UNC2170 is able to compete with Kme2 peptide substrates for binding, H4K20me2 and p53K382me2 peptide pull down assays were conducted. UNC2170 was able to successfully displace the tandem tudor domain of a His-53BP1 fusion protein from both H4K20me2 and p53K382me2 peptides (Figure 3a). Additionally, UNC2170 displaces His-53BP1 from immobilized p53K382me2 in a dose dependent fashion (Figure 3b), resulting in an apparent IC_{50} of about 30 μM which is consistent with the results from other *in vitro* assays described above.

Additional chromatin release assays were conducted in HEK293 cell lysates to determine if UNC2170 could influence the amount of endogenous 53BP1 bound to chromatin. Purification of chromatin from HEK293 cells was followed by compound treatment for two hours at room temperature and subsequent separation of the solubilized proteins from those remaining on chromatin. Western blot analysis revealed that treatment with UNC2170 (500 μM) resulted in a significant increase in soluble 53BP1 as compared to untreated lysates or lysates treated with UNC2892, the negative control compound (Figure 4a). This effect was found to be concentration dependent, as an increase in soluble 53BP1 was observed with increasing concentrations of UNC2170 (Figure 4b), and partial release of 53BP1 was detected at concentrations as low as 10 μM. This result is consistent with UNC2170 antagonizing the interaction between the tudor domain of full-length 53BP1 and chromatin.

We next sought to evaluate the potential of UNC2170 to engage 53BP1 in a cellular context. The low molecular weight (313.24 g/mol) and clogP (~3.27) of UNC2170 suggested *a priori* that UNC2170 would be cell permeant. To confirm this and assess the suitability of the compound for cell studies, the cell permeability of UNC2170 was determined. We found that UNC2170 was indeed highly cell permeant with no significant measureable cellular efflux (efflux ratio = 1.2) as determined by a bi-directional Caco-2 cell permeability assay.(47) Furthermore, UNC2170 has no measurable toxicity within the desired concentrations for cellular experiments, with cell toxicity only beginning to take effect at >10 mM as measured by a CellTiter-Glo luminescent cell-viability assay (Supplementary Figure S4).

Although the tandem tudor domains of 53BP1 are required for foci formation after ionizing radiation,(23) pretreatment of U2OS cells with UNC2170 (1 hour, 100 – 300 μM) did not significantly decrease the extent of endogenous 53BP1 foci formed following 5 Gy irradiation, and similar results were observed with UNC2982 (Supplementary Figure S5). To further support this, γH2AX foci were also quantified after compound treatment and no changes were observed. In addition, UNC2170 did not affect the apparent residence time of a GFP fusion protein containing the 53BP1 tudor domains as measured by fluorescence recovery after photobleaching (FRAP) experiments before or after ionizing radiation (10 Gy). Recent evidence suggesting that 53BP1 is a bivalent histone modification reader due to its recognition of H2AK15ub by its ubiquitination-dependent recruitment (UDR) modif(27) is one possible explanation for the maintenance of 53BP1 recruitment to DSB sites upon treatment with UNC2170 in these assays. Overall, UNC2170 treatment does not appear to be

Author Manuscript Author Manuscript Author Manuscript Author Manuscript

sufficient to block 53BP1 recruitment after ionizing radiation and a more potent ligand may be required for such activity.

As efficient B cell antibody class switch recombination (CSR) requires 53BP1 to have an active tudor domain and 53BP1 knockout mice are severely impaired in their ability to undergo CSR,(48, 49) we sought to determine whether UNC2170 would induce this same defect. Naive IgM^+ B cells were stimulated to undergo isotype switching to IgG1 with LPS and Il-4, treated with UNC2170, UNC2892, or mock treated, and then the relative switching to IgG1 was determined by FACS analysis 3.5 days after compound treatment. B cells treated with UNC2170 (75 μM) underwent CSR 64% as effectively as untreated cells (Figure 5, Supplementary Figure S6), while treatment with UNC2892 had a much less significant inhibitory effect on CSR (89%). Although slightly higher and lower doses were tested (100 μM and 30 μM, respectively), treatment at 75 μM appears to be optimal in that the effects observed are specific to the active compound. Our attempts to probe the effect on CSR upon treatment with 300 μM of UNC2170 were unsuccessful, as this resulted in a reduction in cell viability. However, this effect could be mechanism related as UNC2892 does not have the same anti-proliferative effects, and B cells undergoing CSR endure a high rate of DNA damage while proliferating rapidly and therefore represent a particularly sensitive cell subset. It has been reported previously that B cells stimulated from mice bearing a single 53BP1 D1518R amino acid substitution (this mutant is equivalent to D1521R in humans) switch at about 10% of wild type levels.(48) While the effect of UNC2170 is not as pronounced, treatment with UNC2170 clearly phenocopies the reduction in CSR seen in 53BP1 mutant B cells.

CONCLUSIONS

We have shown that the 53BP1 ligand, UNC2170, while only modestly potent, demonstrates at least 17-fold selectivity for 53BP1 as compared to nine other Kme reader proteins. The binding of UNC2170 is also dependent upon a functional tudor domain as demonstrated by site directed mutagenesis and ITC studies. A co-crystal structure revealed that the small molecule ligand binds within the same Kme binding pocket as endogenous Kme peptides. However, distinct from Kme peptide ligands, UNC2170 engages the binding pockets of two 53BP1 tudor domains. This simple, relatively non-toxic ligand also exhibits modest activity as a 53BP1 antagonist in cellular lysates and has functional consequences in CSR assays consistent with its weak *in vitro* activity. A closely related negative control compound, UNC2892, lacks both *in vitro* and cellular effects, suggesting that the results observed with UNC2170 are indeed due to the inhibition of 53BP1. Thus, UNC2170 is a novel small molecule ligand of 53BP1, a Kme reader protein that has gained much attention recently due to its integral role in DNA damage repair and its link to BRCA1. Our preliminary SAR studies revealed only modest improvements in potency, and further exploitation of the structural data should facilitate the development of a high-quality chemical probe for 53BP1. This work also aids in demonstrating the potential for Kme readers to be modulated via small molecule intervention, despite the limited research in this field to date.

Author Manuscript Author Manuscript Author Manuscript Author Manuscript

METHODS

AlphaScreen

The AlphaScreen assay was generally performed as previously described.(37) In brief, compound plates (1 μL at 10 mM highest concentration; 3-fold, 10-point dilutions in DMSO) were diluted in 1× assay buffer (20 mM TRIS pH 8.0, 25 mM NaCl, 2 mM DTT and 0.05% Tween-20) to 1 mM using a Multimek robotic pipettor (Nanoscreen) and 1 μL was spotted into the wells of 384-well low-volume Proxiplates (PerkinElmer). To these plates 9 μL of protein-peptide mix in 1× assay buffer was added by Multidrop (Thermo) to bring the final compound concentration to 100 μM and incubated for 30 min at room temperature. Next, 2 μL of a 1:1 mixture of streptavidin-conjugate donor and nickel-chelate acceptor beads (45 μg/mL in 1× assay buffer) were added and the plates were allowed to incubate for an additional 30 min in the dark at room temperature. After incubation, the plates were read on an EnVision multi-label reader equipped with an HTS AlphaScreen laser (Perkin Elmer). The IC_{50} values reported are the average of at least 3 values ± the standard deviation. When IC_{50} values for a single compound were not all active (< 100 μM) or inactive (> 100 μM), the IC_{50} values were calculated using 4-paramter curve fitting (GraphPad Prism 5) from replicate runs using averaged response values for each compound concentration.

Chromatin Fractionation Experiments

Chromatin was isolated from HEK293 cells. Cells were lysed in EBC-1 buffer (Tris pH 7.5, 100mM NaCl, 0.5% NP-40, 1mM EDTA), nuclear pellets were collected, washed in EBC-1 and resuspended in EBC-2 (Tris pH7.5, 300mM NaCl, 5mM CaCl2) for 30 minutes. The insoluble chromatin was pelleted and resuspended in EBC-2 for use in the release assay. This chromatin was incubated with the indicated concentration of compounds for 2 hrs at RT. The supernatant was collected and analyzed as the soluble fraction while the remaining pellet was resuspended in loading buffer, sonicated, and analyzed as the chromatin bound fraction. Anti-53BP1 (Sigma B4436) and anti-histone 3 (loading control) were used in western blots.

Crystallization

Purified 53BP1 (42 mg/mL) in 20 mM HEPES, pH 7.5, 150 mM NaCl, 0.5 mM TCEP was pre-incubated with 10 mM UNC2170 (dissolved in water) and the best crystals were obtained by vapor diffusion technique at 20 °C in sitting drops by mixing 1 μL of protein solution with 1 μL of reservoir solution containing 19% PEG3350, 150 mM DL-malic acid pH 7.2. For cryoprotection, the crystals were soaked in the reservoir solution supplemented with 15% ethylene glycol (v/v) for 60 s before flash freezing in liquid N_2.

CSR Experiments

B cell isolation and culture have been previously described.(50) In brief, primary naive B-lymphocytes from WT C57/BL6 mouse spleens were purified by negative selection with anti-CD43 beads (Miltenyi Biotec) and cultured in RPMI 1640, 1 mM sodium pyruvate, 10% fetal bovine serum (Atlanta Biologicals,), 50 uM 2-mercaptoethanol, 25 μg/ml

Author Manuscript Author Manuscript Author Manuscript Author Manuscript

Lipopolysaccharide(LPS) and 5 ng/ml IL-4 (Sigma-Aldrich). Inhibitors were added at 12 hours culture and cells were analyzed 72 hours later. Cultured splenocytes were stained with anti–mouse IgG1 antibodies (BD). Dead cells were excluded on the basis of forward-side scatter and propidium iodide staining. Cells were analyzed on a LSRFortessa (BD) and data was analyzed with FloJo software. Data is the summary of triplicate culture analysis of 100uM (n=4), 75uM (n=3) and 30uM (n=3) independent experiments. Statistical significance was determined by a two-tailed Student's *t* test assuming unequal variance, p values indicated.

Supplementary Material

Refer to Web version on PubMed Central for supplementary material.

ACKNOWLEDGMENTS

We thank E. Hull-Ryde and N. Cheng for support with the CellTiter-Glo cell viability assay and G. Wang for providing PHF1, PHF19, PHF23, and JARID1A protein constructs. We thank M. Bedford for helpful discussions. The research described here was supported by the National Institute of General Medical Sciences, US National Institutes of Health (NIH, grant R01GM100919), the Carolina Partnership and the University Cancer Research Fund, University of North Carolina at Chapel Hill, and the Welch Foundation (G-1847). The SGC is a registered charity (no. 1097737) that receives funds from AbbVie, Boehringer Ingelheim, the Canada Foundation for Innovation (CFI), the Canadian Institutes of Health Research (CIHR), Genome Canada, Ontario Genomics Institute Grant OGI-055, GlaxoSmithKline, Janssen, Lilly Canada, the Novartis Research Foundation, the Ontario Ministry of Economic Development and Innovation, Pfizer, Takeda, and Wellcome Trust Grant 092809/Z/10/Z. G.M. acknowledges support from NIH grant R01 CA132878 and Mayo Clinic NCI SPORE programs P50 CA116201 and P50 CA108961. G.C. is supported by a Mayo Clinic Cancer Center Fraternal Order of Eagles Fellowship. B.D.S. acknowledges support from the W.M. Keck Foundation. S.B.R. acknowledges support from NIH grant K99CA181343.

ABBREVIATIONS

Kme	methyl-lysine
Kme2	dimethyl-lysine
H4K20me2	histone H4, lysine 20 dimethyl
H4K20me1-2	mono- or dimethylation of lysine 20 on histone 4
SAR	structure activity relationships
PTM	post-translational modification
53BP1	Tumor suppressor p53 binding protein 1
PHD	Plant homeodomain
MBT	malignant brain tumor
L3MBTL3	Lethal(3)malignant brain tumor-like protein 3
L3MBTL1	Lethal(3)malignant brain tumor-like protein 1
MBTD1	MBT domain containing 1
PHF1	PHD finger protein 1
PHF19	PHD finger protein 19

Author Manuscript Author Manuscript Author Manuscript Author Manuscript

PHD23	PHD finger 23
JARID1A	Lysine (K)-specific demethylase 5A
CBX7	Chromobox homolog 7
UHRF1-TTD	Ubiquitin-like, containing PHD and RING finger domains, 1- tandem tudor domain
UHRF1-TTD	Ubiquitin-like, containing PHD and RING finger domains, 1- tandem tudor domain + PHD finger domain
ITC	isothermal titration calorimetry
DDR	DNA Damage Response
CSR	Class Switch Recombination.

REFERENCES

1. Huang J, Berger SL. The emerging field of dynamic lysine methylation of non-histone proteins. Current opinion in genetics & development. 2008; 18:152–158. [PubMed: 18339539]
2. Strahl BD, Allis CD. The language of covalent histone modifications. Nature. 2000; 403:41–45. [PubMed: 10638745]
3. Jenuwein T, Allis CD. Translating the histone code. Science. 2001; 293:1074–1080. [PubMed: 11498575]
4. Jackson SP, Bartek J. The DNA-damage response in human biology and disease. Nature. 2009; 461:1071–1078. [PubMed: 19847258]
5. Kelly TK, De Carvalho DD, Jones PA. Epigenetic modifications as therapeutic targets. Nature biotechnology. 2010; 28:1069–1078.
6. Portela A, Esteller M. Epigenetic modifications and human disease. Nature biotechnology. 2010; 28:1057–1068.
7. Shibata A, Barton O, Noon AT, Dahm K, Deckbar D, Goodarzi AA, Lobrich M, Jeggo PA. Role of ATM and the damage response mediator proteins 53BP1 and MDC1 in the maintenance of G(2)/M checkpoint arrest. Mol Cell Biol. 2010; 30:3371–3383. [PubMed: 20421415]
8. Stewart GS, Wang B, Bignell CR, Taylor AM, Elledge SJ. MDC1 is a mediator of the mammalian DNA damage checkpoint. Nature. 2003; 421:961–966. [PubMed: 12607005]
9. Di Virgilio M, Callen E, Yamane A, Zhang W, Jankovic M, Gitlin AD, Feldhahn N, Resch W, Oliveira TY, Chait BT, Nussenzweig A, Casellas R, Robbiani DF, Nussenzweig MC. Rif1 prevents resection of DNA breaks and promotes immunoglobulin class switching. Science. 2013; 339:711–715. [PubMed: 23306439]
10. Escribano-Diaz C, Orthwein A, Fradet-Turcotte A, Xing M, Young JT, Tkac J, Cook MA, Rosebrock AP, Munro M, Canny MD, Xu D, Durocher D. A cell cycle-dependent regulatory circuit composed of 53BP1-RIF1 and BRCA1-CtIP controls DNA repair pathway choice. Molecular cell. 2013; 49:872–883. [PubMed: 23333306]
11. Sartori AA, Lukas C, Coates J, Mistrik M, Fu S, Bartek J, Baer R, Lukas J, Jackson SP. Human CtIP promotes DNA end resection. Nature. 2007; 450:509–514. [PubMed: 17965729]
12. Mochan TA, Venere M, DiTullio RA Jr, Halazonetis TD. 53BP1 and NFBD1/MDC1-Nbs1 function in parallel interacting pathways activating ataxia-telangiectasia mutated (ATM) in response to DNA damage. Cancer research. 2003; 63:8586–8591. [PubMed: 14695167]
13. Kousholt AN, Fugger K, Hoffmann S, Larsen BD, Menzel T, Sartori AA, Sorensen CS. CtIP-dependent DNA resection is required for DNA damage checkpoint maintenance but not initiation. The Journal of cell biology. 2012; 197:869–876. [PubMed: 22733999]

Author Manuscript Author Manuscript Author Manuscript Author Manuscript

14. Zimmermann M, Lottersberger F, Buonomo SB, Sfeir A, de Lange T. 53BP1 regulates DSB repair using Rif1 to control 5' end resection. Science. 2013; 339:700–704. [PubMed: 23306437]
15. Bekker-Jensen S, Lukas C, Melander F, Bartek J, Lukas J. Dynamic assembly and sustained retention of 53BP1 at the sites of DNA damage are controlled by Mdc1/NFBD1. The Journal of cell biology. 2005; 170:201–211. [PubMed: 16009723]
16. Huen MS, Grant R, Manke I, Minn K, Yu X, Yaffe MB, Chen J. RNF8 transduces the DNA-damage signal via histone ubiquitylation and checkpoint protein assembly. Cell. 2007; 131:901–914. [PubMed: 18001825]
17. Doil C, Mailand N, Bekker-Jensen S, Menard P, Larsen DH, Pepperkok R, Ellenberg J, Panier S, Durocher D, Bartek J, Lukas J, Lukas C. RNF168 binds and amplifies ubiquitin conjugates on damaged chromosomes to allow accumulation of repair proteins. Cell. 2009; 136:435–446. [PubMed: 19203579]
18. Ramachandran S, Chahwan R, Nepal RM, Frieder D, Panier S, Roa S, Zaheen A, Durocher D, Scharff MD, Martin A. The RNF8/RNF168 ubiquitin ligase cascade facilitates class switch recombination. Proceedings of the National Academy of Sciences of the United States of America. 2010; 107:809–814. [PubMed: 20080757]
19. Chowdhury D, Keogh MC, Ishii H, Peterson CL, Buratowski S, Lieberman J. gamma-H2AX dephosphorylation by protein phosphatase 2A facilitates DNA double-strand break repair. Molecular cell. 2005; 20:801–809. [PubMed: 16310392]
20. Ward IM, Minn K, van Deursen J, Chen J. p53 Binding protein 53BP1 is required for DNA damage responses and tumor suppression in mice. Mol Cell Biol. 2003; 23:2556–2563. [PubMed: 12640136]
21. Narod SA. BRCA mutations in the management of breast cancer: the state of the art. Nature reviews. Clinical oncology. 2010; 7:702–707.
22. Manis JP, Morales JC, Xia Z, Kutok JL, Alt FW, Carpenter PB. 53BP1 links DNA damage-response pathways to immunoglobulin heavy chain class-switch recombination. Nat Immunol. 2004; 5:481–487. [PubMed: 15077110]
23. Iwabuchi K, Basu BP, Kysela B, Kurihara T, Shibata M, Guan D, Cao Y, Hamada T, Imamura K, Jeggo PA, Date T, Doherty AJ. Potential role for 53BP1 in DNA end-joining repair through direct interaction with DNA. J Biol Chem. 2003; 278:36487–36495. [PubMed: 12824158]
24. Kim J, Daniel J, Espejo A, Lake A, Krishna M, Xia L, Zhang Y, Bedford MT. Tudor, MBT and chromo domains gauge the degree of lysine methylation. EMBO Rep. 2006; 7:397–403. [PubMed: 16415788]
25. Botuyan MV, Lee J, Ward IM, Kim J-E, Thompson JR, Chen J, Mer G. Structural Basis for the Methylation State-Specific Recognition of Histone H4-K20 by 53BP1 and Crb2 in DNA Repair. Cell. 2006; 127:1361–1373. [PubMed: 17190600]
26. Kachirskaia I, Shi X, Yamaguchi H, Tanoue K, Wen H, Wang EW, Appella E, Gozani O. Role for 53BP1 Tudor domain recognition of p53 dimethylated at lysine 382 in DNA damage signaling. J Biol Chem. 2008; 283:34660–34666. [PubMed: 18840612]
27. Fradet-Turcotte A, Canny MD, Escribano-Diaz C, Orthwein A, Leung CC, Huang H, Landry MC, Kitevski-LeBlanc J, Noordermeer SM, Sicheri F, Durocher D. 53BP1 is a reader of the DNA-damage-induced H2A Lys 15 ubiquitin mark. Nature. 2013; 499:50–54. [PubMed: 23760478]
28. Acs K, Luijsterburg MS, Ackermann L, Salomons FA, Hoppe T, Dantuma NP. The AAA-ATPase VCP/p97 promotes 53BP1 recruitment by removing L3MBTL1 from DNA double-strand breaks. Nat Struct Mol Biol. 2011; 18:1345–1350. [PubMed: 22120668]
29. Mallette FA, Mattiroli F, Cui G, Young LC, Hendzel MJ, Mer G, Sixma TK, Richard S. RNF8- and RNF168-dependent degradation of KDM4A/JMJD2A triggers 53BP1 recruitment to DNA damage sites. EMBO J. 2012
30. Roy R, Chun J, Powell SN. BRCA1 and BRCA2: different roles in a common pathway of genome protection. Nat Rev Cancer. 2012; 12:68–78. [PubMed: 22193408]
31. Hakem R, de la Pompa JL, Sirard C, Mo R, Woo M, Hakem A, Wakeham A, Potter J, Reitmair A, Billia F, Firpo E, Hui CC, Roberts J, Rossant J, Mak TW. The tumor suppressor gene Brca1 is required for embryonic cellular proliferation in the mouse. Cell. 1996; 85:1009–1023. [PubMed: 8674108]

Author Manuscript Author Manuscript Author Manuscript Author Manuscript

32. Xu X, Wagner KU, Larson D, Weaver Z, Li C, Ried T, Hennighausen L, Wynshaw-Boris A, Deng CX. Conditional mutation of Brca1 in mammary epithelial cells results in blunted ductal morphogenesis and tumour formation. Nat Genet. 1999; 22:37–43. [PubMed: 10319859]
33. Cao L, Xu X, Bunting SF, Liu J, Wang RH, Cao LL, Wu JJ, Peng TN, Chen J, Nussenzweig A, Deng CX, Finkel T. A selective requirement for 53BP1 in the biological response to genomic instability induced by Brca1 deficiency. Molecular cell. 2009; 35:534–541. [PubMed: 19716796]
34. Bunting SF, Callen E, Wong N, Chen HT, Polato F, Gunn A, Bothmer A, Feldhahn N, Fernandez-Capetillo O, Cao L, Xu X, Deng CX, Finkel T, Nussenzweig M, Stark JM, Nussenzweig A. 53BP1 inhibits homologous recombination in Brca1-deficient cells by blocking resection of DNA breaks. Cell. 2010; 141:243–254. [PubMed: 20362325]
35. Cui G, Botuyan MV, Mer G. Preparation of recombinant peptides with site- and degree-specific lysine (13)C-methylation. Biochemistry. 2009; 48:3798–3800. [PubMed: 19334741]
36. Tang J, Cho NW, Cui G, Manion EM, Shanbhag NM, Botuyan MV, Mer G, Greenberg RA. Acetylation limits 53BP1 association with damaged chromatin to promote homologous recombination. Nat Struct Mol Biol. 2013; 20:317–325. [PubMed: 23377543]
37. Wigle TJ, Herold JM, Senisterra GA, Vedadi M, Kireev DB, Arrowsmith CH, Frye SV, Janzen WP. Screening for inhibitors of low-affinity epigenetic peptide-protein interactions: an AlphaScreen-based assay for antagonists of methyl-lysine binding proteins. J Biomol Screen. 2010; 15:62–71. [PubMed: 20008125]
38. Shultz MD. Setting expectations in molecular optimizations: Strengths and limitations of commonly used composite parameters. Bioorganic & medicinal chemistry letters. 2013; 23:5980–5991. [PubMed: 24018190]
39. Reynolds CH, Tounge BA, Bembenek SD. Ligand binding efficiency: trends, physical basis, and implications. Journal of medicinal chemistry. 2008; 51:2432–2438. [PubMed: 18380424]
40. Frye SV. The art of the chemical probe. Nature chemical biology. 2010; 6:159–161.
41. James LI, Korboukh VK, Krichevsky L, Baughman BM, Herold JM, Norris JL, Jin J, Kireev DB, Janzen WP, Arrowsmith CH, Frye SV. Small-Molecule Ligands of Methyl-Lysine Binding Proteins: Optimization of Selectivity for L3MBTL3. J Med Chem. 2013; 56:7358–7371. [PubMed: 24040942]
42. James LI, Barsyte-Lovejoy D, Zhong N, Krichevsky L, Korboukh VK, Herold JM, MacNevin CJ, Norris JL, Sagum CA, Tempel W, Marcon E, Guo H, Gao C, Huang XP, Duan S, Emili A, Greenblatt JF, Kireev DB, Jin J, Janzen WP, Brown PJ, Bedford MT, Arrowsmith CH, Frye SV. Discovery of a chemical probe for the L3MBTL3 methyllysine reader domain. Nature chemical biology. 2013; 9:184–191.
43. Herold JM, Wigle TJ, Norris JL, Lam R, Korboukh VK, Gao C, Ingerman LA, Kireev DB, Senisterra G, Vedadi M, Tripathy A, Brown PJ, Arrowsmith CH, Jin J, Janzen WP, Frye SV. Small-molecule ligands of methyl-lysine binding proteins. Journal of medicinal chemistry. 2011; 54:2504–2511. [PubMed: 21417280]
44. Kireev D, Wigle TJ, Norris-Drouin J, Herold JM, Janzen WP, Frye SV. Identification of Non-Peptide Malignant Brain Tumor (MBT) Repeat Antagonists by Virtual Screening of Commercially Available Compounds. J Med Chem. 2010; 53:7625–7631. [PubMed: 20931980]
45. Herold JM, James LI, Korboukh VK, Gao C, Coil KE, Bua DJ, Norris JL, Kireev DB, Brown PJ, Jin J, Janzen WP, Gozani O, Frye SV. Structure-activity relationships of methyl-lysine reader antagonists. Med chem comm. 2012; 3:45–51.
46. Wilcken R, Zimmermann MO, Lange A, Zahn S, Boeckler FM. Using halogen bonds to address the protein backbone: a systematic evaluation. Journal of computer-aided molecular design. 2012; 26:935–945. [PubMed: 22865255]
47. Smart OS, Womack TO, Sharff A, Flensburg C, Keller P, Paciorek W, Vonrhein C, Bricogne G. Global Phasing Ltd. 2011
48. Bothmer A, Robbiani DF, Di Virgilio M, Bunting SF, Klein IA, Feldhahn N, Barlow J, Chen HT, Bosque D, Callen E, Nussenzweig A, Nussenzweig MC. Regulation of DNA end joining, resection, and immunoglobulin class switch recombination by 53BP1. Molecular cell. 2011; 42:319–329. [PubMed: 21549309]

Author Manuscript Author Manuscript Author Manuscript Author Manuscript

49. Ward IM, Reina-San-Martin B, Olaru A, Minn K, Tamada K, Lau JS, Cascalho M, Chen L, Nussenzweig A, Livak F, Nussenzweig MC, Chen J. 53BP1 is required for class switch recombination. The Journal of cell biology. 2004; 165:459–464. [PubMed: 15159415]

50. Gazumyan A, Timachova K, Yuen G, Siden E, Di Virgilio M, Woo EM, Chait BT, Reina San-Martin B, Nussenzweig MC, McBride KM. Amino-terminal phosphorylation of activation-induced cytidine deaminase suppresses c-myc/IgH translocation. Mol Cell Biol. 2011; 31:442–449. [PubMed: 21135131]

Author Manuscript Author Manuscript Author Manuscript Author Manuscript

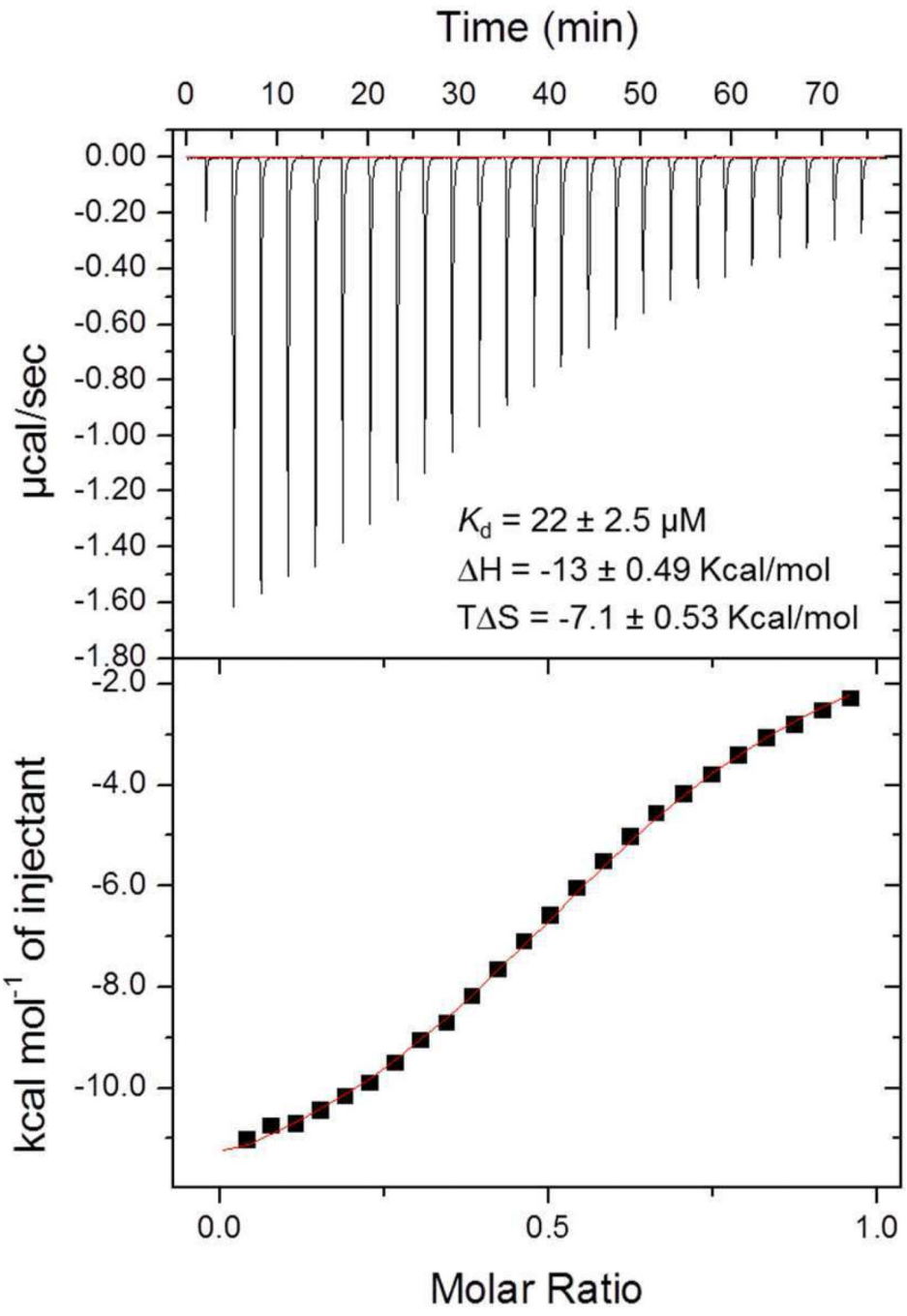

Figure 1.
ITC analysis of 53BP1 binding to UNC2170 (**1**), revealing a K_d of 22 ± 2.5 µM.

Author Manuscript Author Manuscript Author Manuscript Author Manuscript

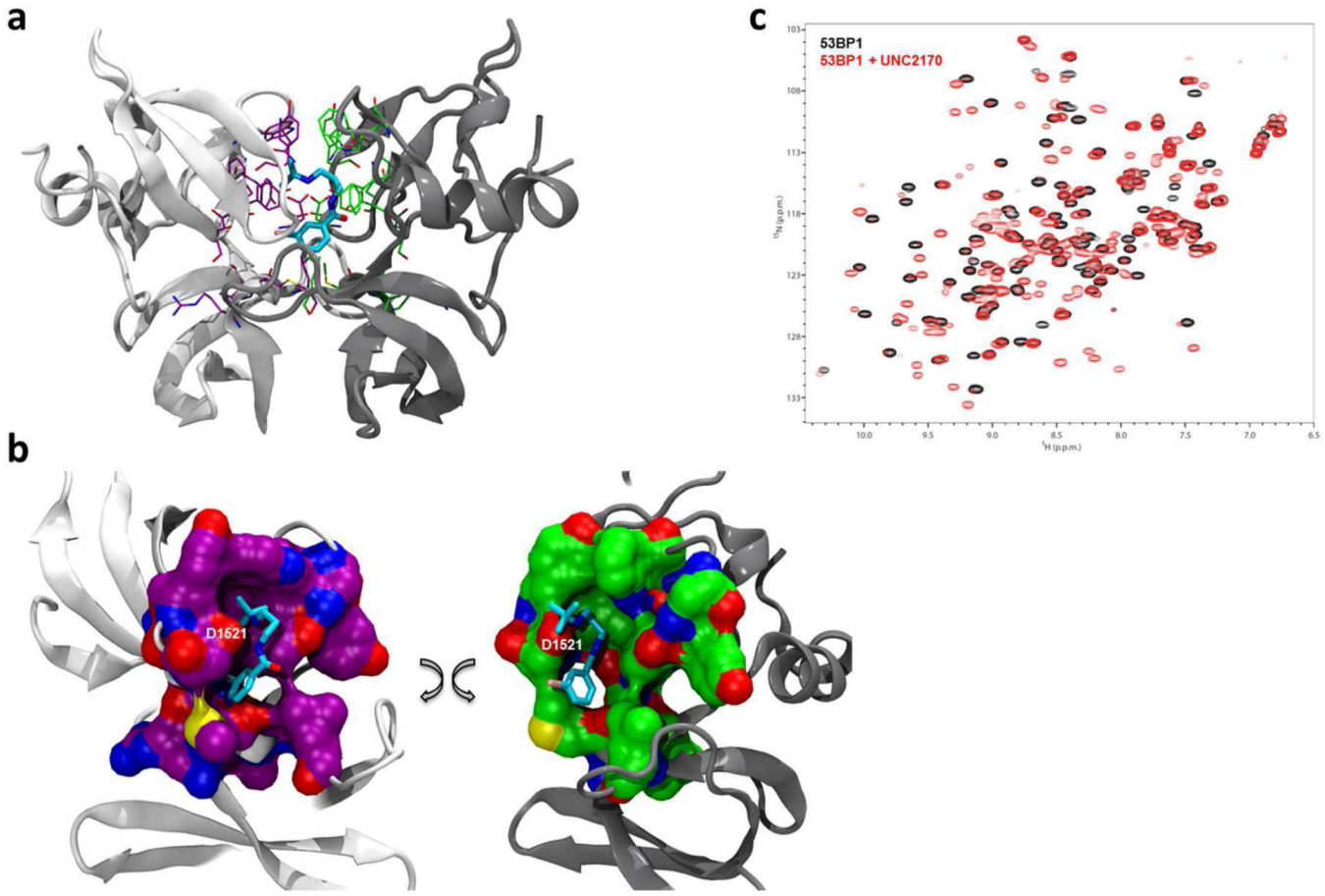

Figure 2.

Crystallography and NMR evidence for UNC2170 (**1**) binding to 53BP1. (a) Co-crystal structure of **1** (cyan) bound to the 53BP1 tudor domain dimer (PDB 4RG2). One 53BP1 protein unit is shown in light gray and the other in dark gray, with the residues that interact with UNC2170 shown in fuchsia and green, respectively. (b) View of the protein surface of each 53BP1 tudor domain that interacts with UNC2170 (the two domains shown in (a) are separated and rotated); color coding is the same as in (a). (c) Overlay of the ^{1}H-^{15}N HSQC correlation spectra of 53BP1 in the free state (black) and in the presence of 10-fold molar excess UNC2170 (red).

Author Manuscript Author Manuscript Author Manuscript Author Manuscript

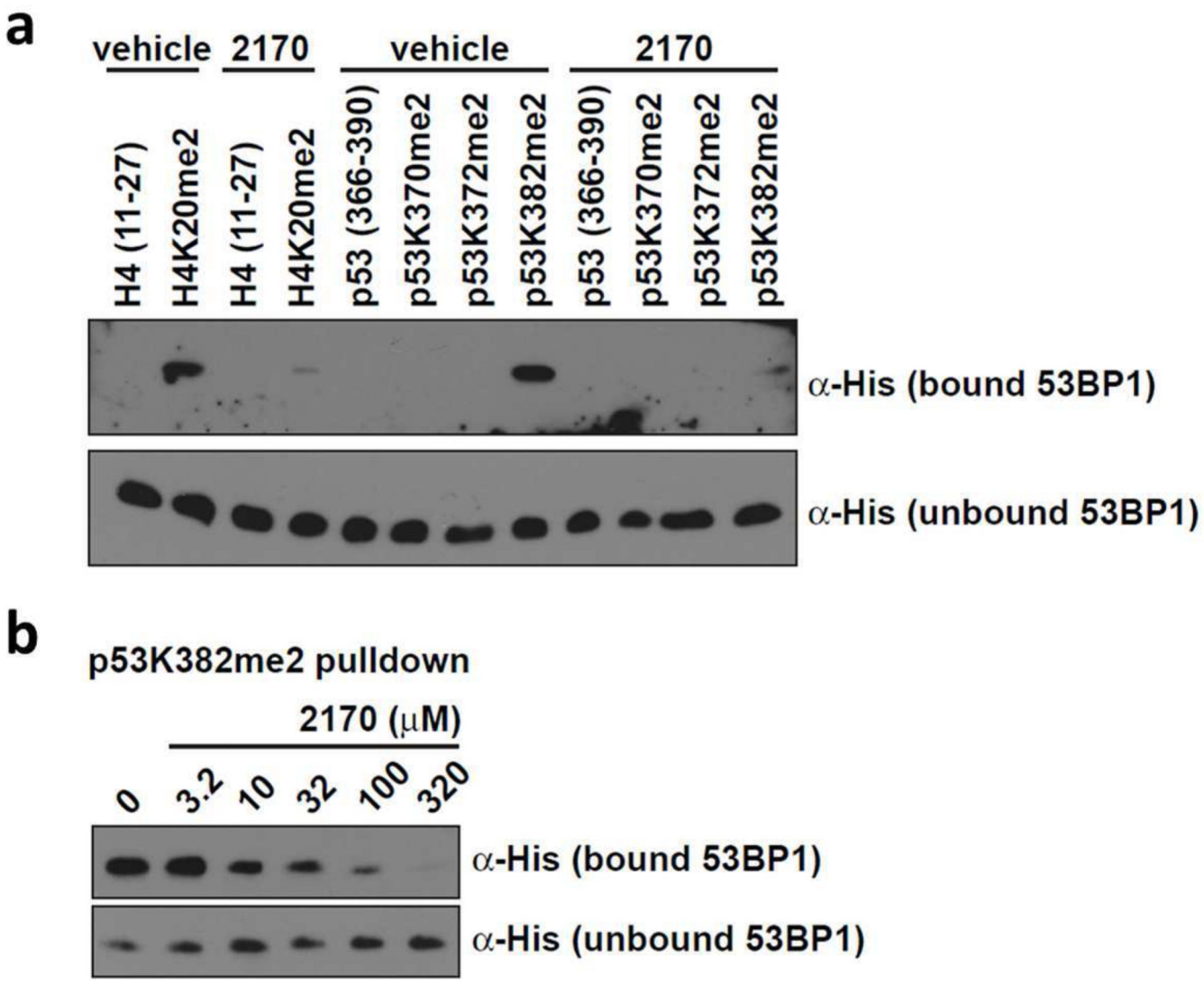

Figure 3.

Western blot analysis following competitive in-solution peptide pulldown assays with His-53BP1 TTD and (a) 500 μM UNC2170 or (b) the indicated concentration of UNC2170 shows inhibition of the interaction between the 53BP1 TTD and H4K20me2 and p53K382me2 peptides. UNC2170 displaces His-53BP1 from immobilized p53K382me2 in a dose dependent fashion.

Author Manuscript Author Manuscript Author Manuscript Author Manuscript

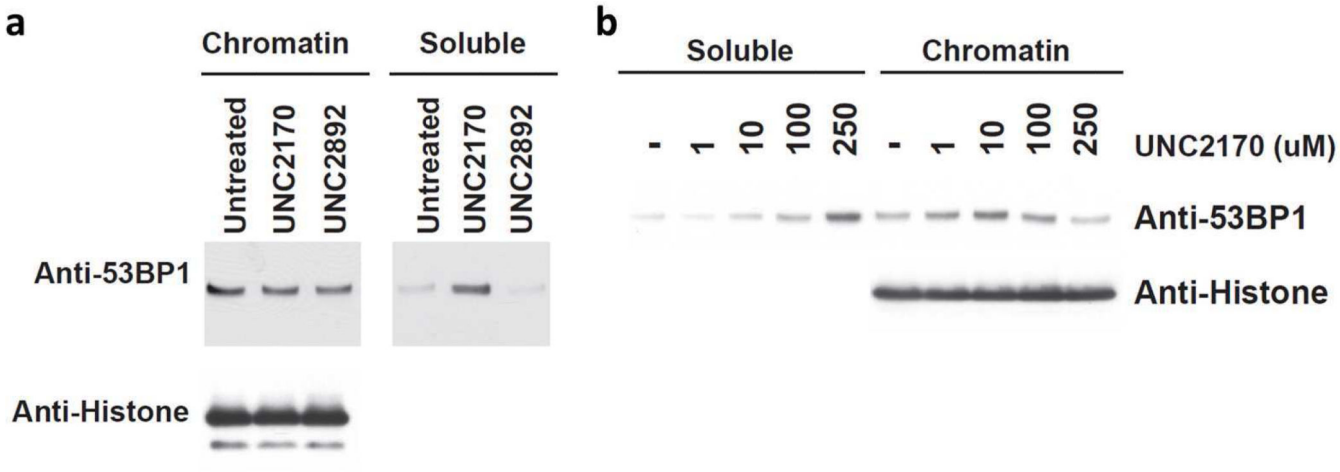

Figure 4.

Western blot analysis of HEK293 cell lysates biochemically separated into chromatin and soluble fractions after treatment with (a) 500 μM UNC2170 or UNC2892 or (b) the indicated concentration of UNC2170 for 2 hours at room temperature. Anti-Histone 3 is shown as an input control.

Author Manuscript Author Manuscript Author Manuscript Author Manuscript

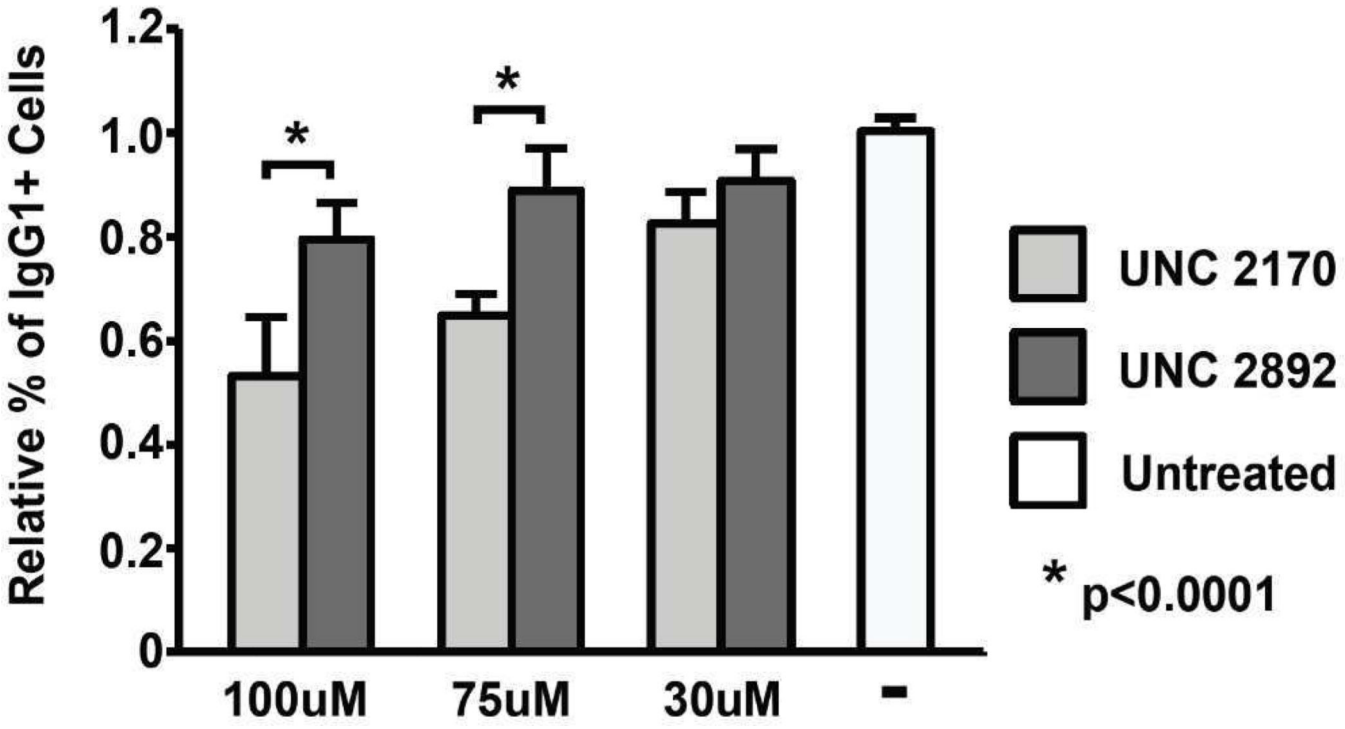

Figure 5.

Summary of relative CSR to IgG1 switching in naive splenocytes cultured with LPS and IL-4 for 3.5 days in the presence of UNC2170 or UNC2892 at the indicated concentrations as compared to untreated cells. Averages represent triplicate cultures from four independent experiments. P value (* $p<0.0001$) was determined by a two-tailed t test assuming unequal variance.

Author Manuscript Author Manuscript Author Manuscript Author Manuscript

ACS Chem Biol. Author manuscript; available in PMC 2016 April 17.

Table 1

Selectivity Data For UNC2170 (**1**) and SAR Studies of the Terminal Amine Group.[a,b]

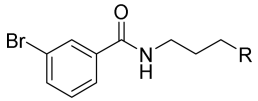

ID	R	53BP1	CBX7	JARID1A	PHF1	PHF19	PHF23	UHRF1	L3MBTL1	L3MBTL3	MBTD1
1[c] (UNC2170)		29 ± 7.4	> 500	> 500	> 500	> 500	> 500	> 500	> 500	> 500	> 500
2		> 100	> 100	> 100	> 100	> 100	> 100	> 100	> 100	> 100	> 100
3		> 100	> 100	> 100	82 ± 13	61 ±0.9	> 100	> 100	> 100	> 100	> 100
4 [c] (UNC2892)		> 500	> 500	> 500	> 500	> 500	> 500	> 500	> 500	> 500	> 500
5	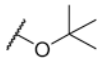	> 100	> 100	> 100	> 100	> 100	> 100	> 100	> 100	> 100	> 100
6		> 100	> 100	> 100	> 100	> 100	> 100	> 100	37 ± 12	> 100	78 ± 16

[a] IC_{50} values are the average of at least 3 values ± the standard deviation as determined by AlphaScreen.

[b] The maximum concentration in the assay was 100 μM and compounds showing less than 50% inhibition at this concentration are labeled >100 μM.

[c] Compounds **1** and **4** were tested at a higher concentration (500 μM) against the panel to further evaluate selectivity.

Author Manuscript Author Manuscript Author Manuscript Author Manuscript

Table 2

SAR Studies of Modifying the Linker of UNC2170.[a,b]

ID	R	53BP1	CBX7	JARID1A	PHF1	PHF19	PHF23	UHRF1	L3MBTL1	L3MBTL3	MBTD1
7	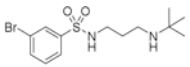	> 100	> 100	> 100	> 100	> 100	> 100	> 100	> 100	> 100	> 100
8	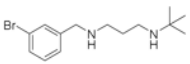	> 100	> 100	> 100	> 100	> 100	> 100	> 100	> 100	> 100	> 100
9	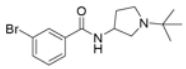	> 100	> 100	> 100	> 100	> 100	> 100	> 100	> 100	> 100	> 100
10	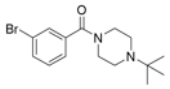	> 100	> 100	> 100	> 100	> 100	> 100	> 100	> 100	> 100	> 100
11	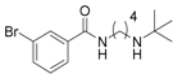	> 100	> 100	> 100	> 100	> 100	> 100	> 100	> 100	> 100	> 100
12	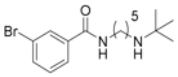	> 100	> 100	> 100	> 100	> 100	> 100	> 100	> 100	> 100	> 100
13	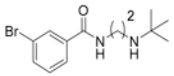	> 100	> 100	> 100	> 100	> 100	> 100	> 100	> 100	> 100	> 100

[a] IC_{50} values are the average of at least 3 values ± the standard deviation as determined by AlphaScreen.

[b] The maximum concentration in the assay was 100 μM and compounds showing less than 50% inhibition at this concentration are labeled >100 μM.

Author Manuscript Author Manuscript Author Manuscript Author Manuscript

Table 3

SAR Studies of the Aromatic Head Group of UNC2170. [a,b]

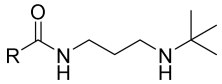

ID	R	53BP1	CBX7	JARID1A	PHF1	PHF19	PHF23	UHRF1	L3MBTL1	L3MBTL3	MBTD1
14		> 100	> 100	> 100	> 100	> 100	> 100	> 100	> 100	> 100	> 100
15	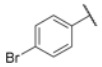	> 100	> 100	> 100	> 100	> 100	> 100	> 100	> 100	> 100	> 100
16		> 100	> 100	> 100	> 100	> 100	> 100	> 100	> 100	> 100	> 100
17	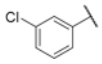	> 100	> 100	> 100	> 100	> 100	> 100	> 100	> 100	> 100	> 100
18	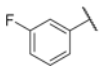	> 100	> 100	> 100	> 100	> 100	> 100	> 100	> 100	> 100	> 100
19		13 ± 4.8	> 100	> 100	> 100	> 100	> 100	> 100	> 100	> 100	> 100
20	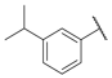	14 ± 7.6	> 100	> 100	> 100	> 100	> 100	> 100	> 100	> 100	> 100
21	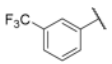	22 ± 14	> 100	> 100	> 100	> 100	> 100	> 100	> 100	> 100	> 100
22	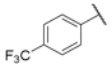	> 100	> 100	> 100	> 100	> 100	> 100	> 100	> 100	> 100	> 100

Author Manuscript Author Manuscript Author Manuscript Author Manuscript

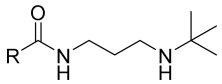

ID	R	53BP1	CBX7	JARID1A	PHF1	PHF19	PHF23	UHRF1	L3MBTL1	L3MBTL3	MBTD1
23	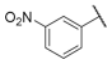	> 100	> 100	> 100	> 100	> 100	> 100	> 100	> 100	> 100	> 100
24	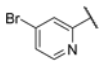	> 100	> 100	> 100	> 100	> 100	> 100	> 100	> 100	> 100	> 100
25	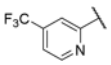	> 100	> 100	> 100	> 100	> 100	> 100	> 100	> 100	> 100	> 100

[a] IC_{50} values are the average of at least 3 values ± the standard deviation as determined by AlphaScreen.

[b] The maximum concentration in the assay was 100 μM and compounds showing less than 50% inhibition at this concentration are labeled >100 μM.